Genetic Improvement of *Clostridium tyrobutyricum* for Butanol Production by Insertion of *adhE* from *Clostridium acetobutylicum*

Honors Thesis

Presented in Partial Fulfillment of the Requirements for the Degree Bachelor of Science with Distinction in the College of Engineering of The Ohio State University

By

Robert Donald Hoelzle

Undergraduate Program in Chemical Engineering

The Ohio State University

2010

Thesis Committee

Shang-Tian Yang, Advisor

James Rathman

Abstract

Butanol, a common fermentation product, has the potential to be a more economically and environmentally friendly biofuel than ethanol. However, current strains capable of fermenting butanol do not produce it in high enough concentrations for the process to be economically feasible. *Clostridium tyrobutyricum* does not naturally produce butanol, but it does produce the metabolic precursors to butanol in *Clostridium acetobutylicum*, the most commonly used butanol-producing strain. The gene *adhE*, one of two genes coding for the alcohol-aldehyde dehydrogenases that produce butanol from these metabolic precursors in *C. acetobutylicum,* along with a powerful constitutive promoter were isolated and amplified for insertion into *C. tyrobutyricum* in order to create a butanol-producing mutant strain. The plasmid transformation protocol is still being optimized, so the final mutant has not yet been created. However, it is reasonable to believe that this mutant, once completed, will be capable of butanol production.

Dedication

This thesis is dedicated to all those who encouraged and inspired me along the way. In particular, to Rachel Merrick, who first encouraged me to pursue this project, and to my Mother, Linda, whose invaluable advice kept me motivated along the way. Thank you so much to all of you, as I would not have finished without you.

Acknowledgements

I would like to send a special thanks to Dr. Shang-Tian Yang for advising me during my research, to Dr. Mingrui Yu for instructing me on laboratory procedures and protocol, and to the rest of the members of Dr. Yang's research team for their insights and assistances.

Vita

May 2004……..Fremont Ross High School

January 2005 to Present……...Undergraduate Education in Chemical and Biomolecular Engineering

Summer 2008……..……Internship at Whirlpool Corporation

August 2009 to Present…….Research in Metabolic Engineering

Fields of Study

Major Field: Chemical and Biomolecular Engineering

Table of Contents

Abstract ii

Dedication iii

Acknowledgements iv

Vita v

List of Tables viii

List of Figures x

List of Abbreviations xii

Chapter 1: Introduction 1

Chapter 2: Literature Review 4

2.1: Butanol 4

2.2: Potential of butanol as a biofuel 5

2.3: Butanol-fermenting bacteria and genes 7

2.4: *Clostridium tyrobutyricum* 10

2.5: Gene transcription promoters 12

Chapter 3: Materials and Methods 13

3.1: Bacterial strains and plasmids 13

3.2: Restriction sites and primer design 15

3.3: DNA amplification, digestion, purification, and ligation 18

3.4: Vector transformation 21

Chapter 4: Results and Discussion 26

Chapter 5: Conclusions 32

Chapter 6: Future Work 35

References 37

Appendix: Reaction Protocols 40

List of Tables

Table 1. Comparison of gasoline, ethanol, and butanol energy contents [3]. 3

Table 2. Thermo-physical property data for butanol. Values obtained from *[22] and **[16]. 4

Table 3. Comparative chemical properties of butanol, ethanol, and gasoline. Values obtained from *[3], **[1, 7, 13], and ***[14]. 6

Table 4. Full factorial experimental layout for optimizing the ligation and transformation process. 29

Table 5. PCR protocol as called for by protocol for Platinum® *Taq* DNA Polymerase High Fidelity. DNA template is replaced by cell colony for colony PCR. 40

Table 6. Temperature cycle for PCR with Platinum® *Taq* DNA Polymerase. 40

Table 7. Ligation of gene PCR product with pGEM®-T vector. 41

Table 8. Ligation of promoter PCR product with pGEM®-T vector. 41

Table 9. Protocol for transformation of all ligation products into DH5 cells. Transformation product was plated and grown as described in Chapter 3. 41

Table 10. Protocol for digestion of pGEM®-T ligation products and pMTL007. *For thiolase promoter, use 55 µl. 41

Table 11. Protocol for ligation of thiolase promoter with pMTL007. This protocol is still being optimized. 41

Table 12. Protocol for making LB plates. *Components only used with pMTL007 recombinant plasmids. **Components only used with pGEM®-T recombinant plasmids. 41

List of Figures

Figure 1. ABE pathway of *Clostridium acetobutylicum*..... 9

Figure 2. Butyrate and acetate producing pathway of *Clostridium tyrobutyricum*..... 11

Figure 3. pMTL007 showing restriction sites for promoter and gene insertion. 14

Figure 4. Layout of the final recombinant plasmid *thl-adhE*-pMTL007..... 16

Figure 5. Sequences of ForAAD and RevAAD. Restriction sites are in bold and underlined with their labels below the site. Restriction points shown with an apostrophe. The start codon is italicized and underlined. 17

Figure 6. Sequences of ForAAD and RevAAD. Restriction sites are in bold and underlined with their labels below the site. Restriction points shown with an apostrophe..... 18

Figure 7. Diagram depicting the creation of the *thl*-pMTL007 recombinant plasmid starting from the *Clostridium tyrobutyricum* genome..... 23

Figure 8. Diagram depicting the creation of the *adhE*-pGEM-T recombinant plasmid starting with pSOL1 from *Clostridium acetobutylicum*..... 24

Figure 9. Diagram depicting the creation of the *thl-adhE*-pMTL007 recombinant plasmid. 25

Figure 10. PCR amplification of the thiolase promoter. Lane 1 is the sizing ladder, lane 2 is the promoter, and all other lanes are empty..... 26

Figure 11. Colony PCR of the thiolase promoter. Lane 1 is the negative control, lanes 2-11 are the colonies, lane 12 is the positive control, lane 13 is the sizing ladder, and the other lanes are empty..... 27

Figure 12. Digestion of the thiolase promoter and pMTL007 with *XhoI* and *SacII*. Lanes 1-3 are the promoter, lane 4 is the sizing ladder, lanes 5 and 6 are pMTL007, and lanes 7 and 8 are empty. 28

Figure 13. Second digestion of the thiolase promoter with *XhoI* and *SacII*. Lanes 2-4 are the promoter, lane 5 is the sizing ladder, and the other lanes are empty. 28

Figure 14. PCR amplification of *adhE*. Lane 1 is the sizing ladder, lane 2 is a failed amplification, lane 3 is a successful amplification, and the other lanes are empty. 30

Figure 15. Colony PCR of *adhE*. Lane 2 is the sizing ladder, lanes 3-12 are the colonies, lane 13 is the positive control, lane 14 is the negative control, all other lanes are empty. 30

List of Abbreviations

AAD	Alcohol-Aldehyde Dehydrogenase
ABE	Acetone-Butanol-Ethanol
bp	Base Pairs
C.	*Clostridium*
Cp	Heat Capacity
ΔG°_{f}	Standard Gibbs Free Energy of Formation
ΔH°_{f}	Standard Enthalpy of Formation
ΔH_{vap}	Latent Heat of Vaporization
E.	*Escherichia*
IPTG	Isopropyl β-D-1-Thiogalactopyranoside
kb	Kilo Base Pairs
MW	Molecular Weight
P_c	Critical Pressure
P_{vap}	Vapor Pressure
ρ	Density
STP	Standard Temperature and Pressure
T_{boil}	Temperature of Boiling
T_c	Critical Temperature
T_{fus}	Temperature of Fusion
V_c	Critical Specific Volume
vol	Volume
X-gal	Bromo-Chloro-Indolyl-Galactopyranoside

Chapter 1: Introduction

Recently, the trends of globalization and population expansion, in addition to technological advances, have led to skyrocketing energy demands worldwide. This is reflected in the transportation industry where increased demand and limited supply of fuel have resulted in vastly inflated prices. Additionally, the increasing demand of petroleum is draining the world's limited oil deposits [31]. While more oil deposits are sure to be found in the future, the fact remains that oil is a non-renewable resource that will eventually run out. Because of this, many institutions around the world are exploring various kinds of renewable and eco-friendly fuels for both the transportation industry and the energy industry as a whole. Current leading technologies for automobiles include electric motors, hydrogen fuel cells, and biofuels.

Electric motors have been around since the dawn of the automobile [25]. However, the electric car fell out of fashion as the gasoline engine became more powerful and more affordable. Governments worldwide have been endorsing the advancement of electric motor technology since the 1980s in response to the looming oil shortage. Research has been focused on extending battery life, increasing power output, and shortening charge time. These are still the main drawbacks to large-scale production today, and while these issues are being improved, electric cars are still reliant on a source of electricity

produced primarily from fossil fuels. This means that the same greenhouse gasses are released by use of an electric car, the gasses just come from the power plant rather than the automobile.

Hydrogen fuel cells have garnered a great deal of attention, as their only exhaust product is steam. However, development is currently at a roadblock due to the use of palladium as the fuel cell's catalyst. Palladium is a very rare and extremely expensive metal, 90% of which is found in remote mines in Russia and South Africa [34]. This would make hydrogen fuel cells more expensive to produce large scale than in the current prototype phase. Another drawback is that the main production source of hydrogen is from fossil fuels [9], meaning that the same problems faced by the gasoline industry now will inevitably affect the production of hydrogen in the future.

Biofuels for small commuter automobiles, such as cars, motorcycles, and small trucks, can be broken down into two groups: ethanol and butanol. Ethanol is currently the major biofuel in production and is derived primarily through fermentation of corn starch [15]. This poses the problem of taking corn from the food supply, which drives up food costs. Additionally, ethanol is energy intensive to produce and only offers about half the energy content of gasoline (Table 1 on page 3). Consequently, ethanol requires a greater energy input to produce than the energy retrieved upon use.

Table 1. Comparison of gasoline, ethanol, and butanol energy contents [3].

Fuel	Energy Content (BTU/gal)
Gasoline	124,340
Ethanol	84,530
Butanol	108,458

Butanol, on the other hand, contains a similar energy content to gasoline (Table 1). It is currently produced as an industrial solvent, primarily as a petroleum derivative. It can also be produced by fermentation of certain strains of bacteria, though in relatively low concentrations [4, 35]. These bacteria can produce butanol from a variety of sugars and, most notably, can ferment plant biowaste such as corn and sugarcane husks. If the fermentation process can be improved to make butanol production economical on the large scale, butanol will be an effective biofuel that is truly environmentally friendly.

Chapter 2: Literature Review

2.1: Butanol

Butanol is an alcohol consisting of a saturated, linear, four-carbon chain and a hydroxyl group on the terminal carbon. It is also known as Butan-1-ol (IUPAC), 1-Butanol, n-Butanol, Butyl alcohol, Butyl hydroxide, Methylolpropane, and Propylcarbinol. It has a molecular formula of $CH_3(CH_2)_2CH_2OH$ and a molecular weight of 74.1216. Its CAS number is 71-36-3. It has a water solubility of 7.7 g/100 ml (1-Butanol) and a viscosity of 2.593 cP at STP [13]. Full thermo-physical property data is listed in Table 2.

Butanol is a clear, colorless, odorless liquid with a mildly alcoholic odor. It is produced

Table 2. Thermo-physical property data for butanol. Values obtained from *[22] and **[16].

Property	Value/Equation , Temperature Range
MW*	74.1216 g/gmol
T_{boil} (1 atm)*	390.6 ± 0.8 K
T_{fus} (1 atm)*	188. ± 9. K
T_c*	562. ± 2. K
P_c*	45. ± 4. bar
V_c*	0.274 l/gmol
$\Delta H°_f$**	-276.96 kJ/gmol
$\Delta G°_f$**	-387.57 kJ/gmol
P_{vap}*	10^(4.54607-(1351.555/(T-93.34)) bar , 295.7 K-390.9 K
	10^(4.39031-(1254.502/(T-105.246)) bar , 391. K-479. K
	10^(4.42921-(1305.001/(T-94.676)) bar , 419.34 K-562.98 K
ρ*	$(0.98279/0.26830)^{(1+(1-T/563.1)^{0.25488})}$ gmol/l , 183.85K-563.10 K
Cp*	$(23.851-9.1292(T/100\ K)+2.7632(T/100\ K)^2)$*8.3143 J/gmol-K , 155. K-490. K
ΔH_{vap}*	$7.1274e-7*(1-T/T_c)^{(0.0483+0.8966*(T/T_c)-0.5116*(T/T_c)^2)}$ J/kgmol , 183.85 K-563.10 K

primarily as petroleum derivative, specifically from propylene, and is a common fermentation product. Butanol is used primarily as an industrial solvent and in the production of butyl esters. It is also used to add artificial flavor to a variety of food products. Additionally, butanol is highly flammable and is an irritant to the eyes, skin, and respiratory tract causing inflammation and dryness [1].

2.2: Potential of butanol as a biofuel

Currently, ethanol is the sole biofuel used to replace and subsidize gasoline for automobile fuel. It is produced by fermentation of biomass using yeast and *Zymomonas mobilis*, as well as by genetically modifying *Escherichia coli* with *Z. mobilis* genes [24]. In 2006, the total world production of bioethanol was 13.5 billion gallons and production is on the rise [15]. While ethanol does help alleviate the need to use non-renewable petroleum and has certain economic benefits, such as creating jobs to handle the increased demand for corn [8], it also has some critical economic drawbacks. In particular, ethanol production requires 29% more energy for production than the energy obtained in combustion when fermented from corn [27], the primary ethanol feedstock used in the United States. This negative net energy gain is due ethanol's relatively low energy content and fermentation yield (2.8 gallons per bushel of corn [15]).

Butanol, while produced in lower quantities than ethanol (2.5 gallons per bushel of corn [26]), has an energy content similar to that of gasoline, and therefore offers more

combustion energy per bushel. Butanol is also more hydrophobic, and therefore less water-soluble, than ethanol, which reduces separation costs. This has several additional effects: it reduces the likelihood that a butanol fuel will stall an engine due to water content; improves the stability of butanol-gasoline mixtures compared to those with ethanol; and lowers nitrogen oxide emissions by lowering the combustion temperature [4]. In depth comparative fuel data for butanol, ethanol, and gasoline is listed in Table 3.

Butanol also has distinct environmental advantages to gasoline. In the summer of 2005, "an *unmodified* '92 Buick [was] driven 10,000 miles across the United States" fueled by 100% butanol [26]. The Buick ran at 20-26 mpg and, on average, reduced hydrocarbons to 95%, carbon monoxide to 97%, nitrogen oxides to 97%, and had a background of 14.7% carbon dioxide, as tested in 10 states. This study proved the ability to use butanol as an energetically and environmentally reliable fuel source given that it is produced in high enough quantities.

Table 3. Comparative chemical properties of butanol, ethanol, and gasoline. Values obtained from *[3], **[1, 7, 13], and ***[14].

Property	Butanol	Ethanol	Gasoline
Energy Content* (BTU/gal)	108,458	84,530	124,340
Solubility in Water** (g/100 ml)	7.7	miscible	0
Flash Point** (˚C)	29	13	< -21
Auto-ignition Temperature** (˚C)	345	363	250
Explosive Limits** (vol % in air)	1.4 - 11.3	3.3 - 19	1.3 - 7.1
Motor Octane Number***	78	102	81 - 89
Viscosity*** (10^{-3} Pa-s)	2.593	1.078	0.24 - 0.32

While butanol currently costs more than both E-85 ethanol blend and standard gasoline ($3.00 per gallon of butanol [26] versus the current national averages of $2.281 per gallon of E-85 and $2.895 per gallon of standard gasoline [2]), the superior environmental performance and the potential to lower butanol costs through enhanced fermentation mean that butanol has great potential as the primary biofuel of the future. Additionally, the ability to use corn as the primary sugar source leads to opportunities to ferment and sell butanol within local markets [26], thereby strengthening local economies in states like Ohio, Nebraska, Iowa, and other corn producing regions. This same idea can be used in regions around the globe that produce any of a variety of high sugar-containing crops.

2.3: Butanol-fermenting bacteria and genes

Butanol, when fermented, is produced by acetone-butanol-ethanol, or ABE, fermentation. This type of fermentation has been well studied since the late 1800's when it was first discovered by Louis Pasteur and was the major production process for acetone and butanol until synthesis from petroleum became more economical in the 1950's [4, 5, 19]. ABE fermentation is performed by certain species of the bacterial genus *Clostridium*, most commonly by *C. acetobutylicum* and *C. beijerinckii* [19]. These bacteria are gram-positive, spore-forming, rod-shaped, obligate anaerobes that are able to ferment a variety of sugars, including glucose and xylose, into the solvents listed above, as well as butyric acid and acetic acid.

C. acetobutylicum ATCC 824 produces butanol from pure glucose by enzymatic activity of *AAD* (alcohol-aldehyde dehydrogenase) and *AAD2*, which are coded for by the genes *adhE* and *adhE2*, respectively [11]. These genes are located on the pSOL1 mega-plasmid, a 192 kb plasmid that is part of ATCC 824's genome, but separate from the main chromosome [23]. The mega-plasmid contains a majority of the genes responsible for ABE fermentation in ATCC 824.

ATCC 824 produces butanol under solventogenic and alcohologenic fermentation conditions in which either *adhE* or *adhE2* is expressed, respectively. Solventogenesis occurs at low pH (~4.4) with standard nutrient availability whereas alcohologenesis occurs near neutral pH when there is high NAD(P)H availability [11]. When near neutral pH with standard nutrient availability, ATCC 824 enters acidogenic fermentation in which it produces primarily acetic acid and butyric acid with little alcohol production; *adhE* is expressed under this condition as well. Solventogenic fermentation produces about 10.3 g/l of butanol [33] whereas alcohologenic fermentation produces only about 5.5 g/l of butanol [11]. Each of the butanol-producing enzymes transforms butyryl-CoA into butanol and, with lower specificity, acetyl-CoA into ethanol (Figure 1 on page 9). Both of these enzymes are active primarily during the stationary phase of fermentation [11].

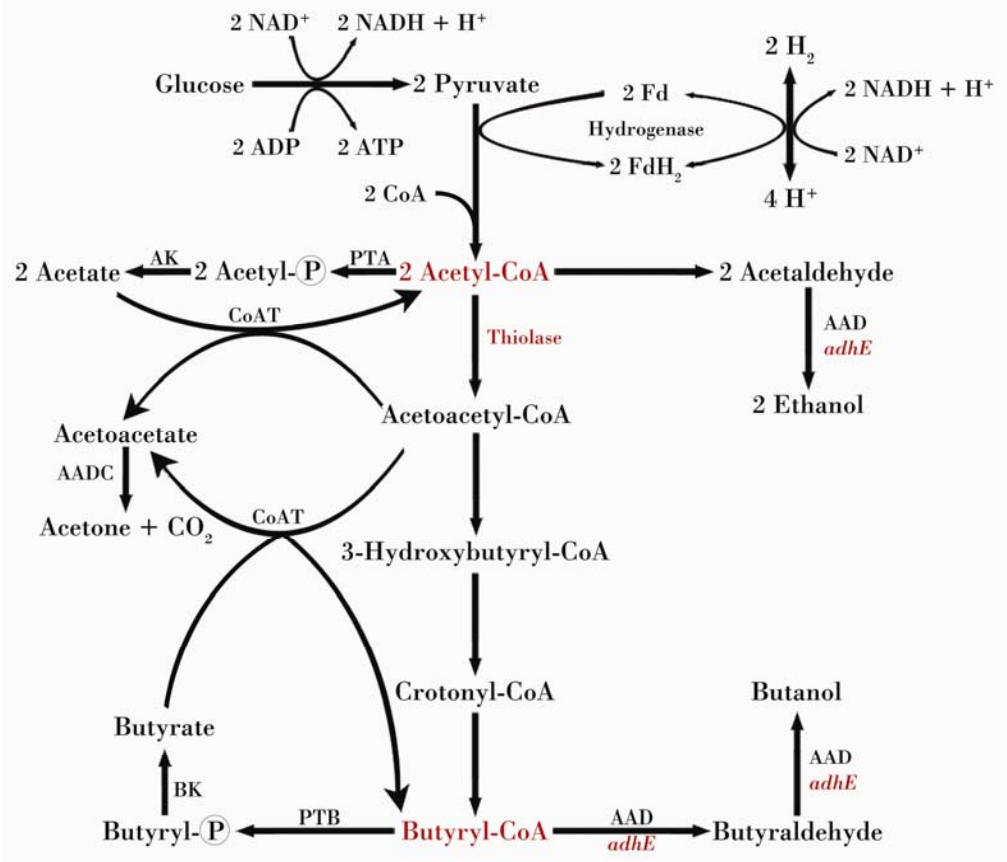

Figure 1. ABE pathway of *Clostridium acetobutylicum*.

Several strains of *C. beijerinckii* are known to produce butanol in high concentrations. These include the wild type NCIMB 8052, the mutant BA101 obtained from NCIMB 8052, and the mutant ATCC 55025 obtained from ATCC 4259 [5, 12, 19, 29]. NCIMB 8052 and ATCC 55025 each produce butanol from pure glucose at final concentrations of about 9 g/l [12, 19] and, like *C. acetobutylicum* ATCC 824, butanol production in these strains occurs during the stationary phase [12]. BA101 produces butanol from pure glucose at a final concentration of about 18 g/l [12]. The reason for the increased level of butanol production is not entirely known, but it may be that the *AAD* enzymes of BA101 are active during both the exponential and stationary phases of fermentation [12].

2.4: *Clostridium tyrobutyricum*

Like *C. acetobutylicum* and *C. beijerinckii*, *C. tyrobutyricum* is a gram-positive, spore-forming, rod-shaped, obligate anaerobe. However, *C. tyrobutyricum* produces only butyric acid, acetic acid, and hydrogen and carbon dioxide gasses by fermentation of glucose and xylose with no alcohol or acetone production [20]. Butyric acid, used as a flavor enhancer, is primarily produced by oxidation of butyraldehyde, a petroleum derivative, though there is increased interest in producing it from biomass for similar reasons as butanol [36]. It is produced through a similar metabolic pathway as butanol in C. acetobutylicum, using the same metabolic precursor: butyryl-CoA (Figure 2, page 11). Optimal production of butyric acid in *C. tyrobutyricum* occurs at about pH 6.3, though smaller amounts of butyric acid are produced at lower pH values (studied down to pH 5.0) [37]. At lower pH values, acetic acid production dominates butyric acid production.

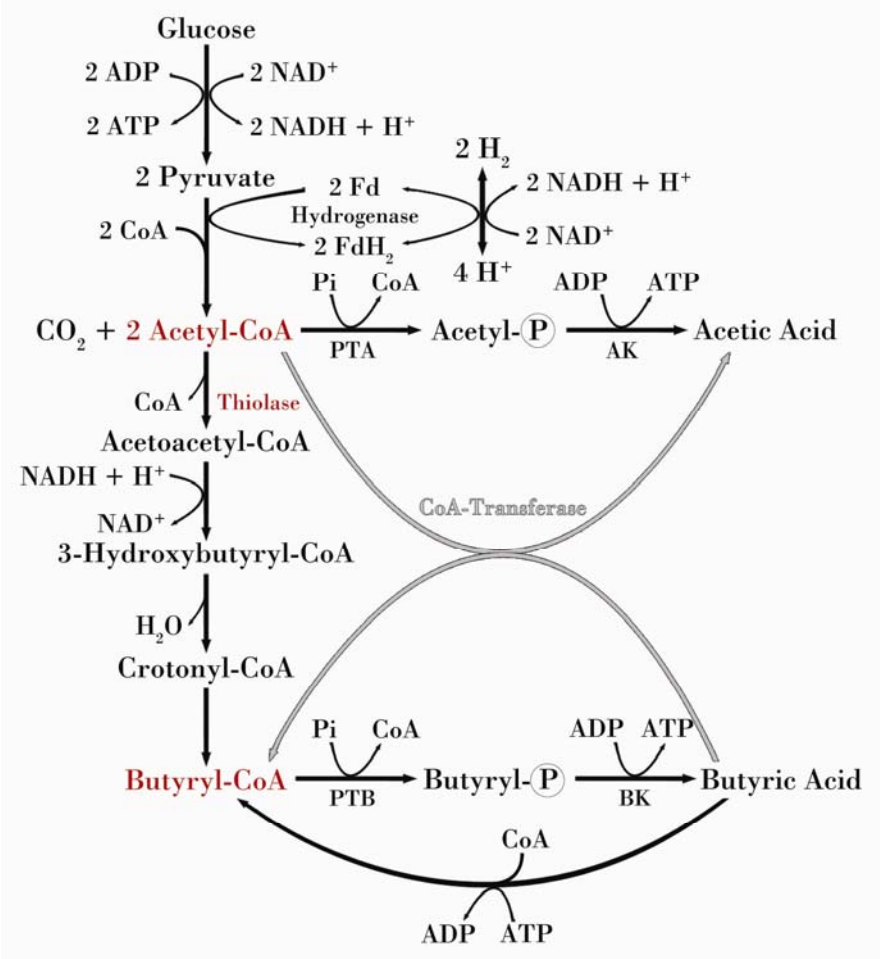

Figure 2. Butyrate and acetate producing pathway of *Clostridium tyrobutyricum*.

It has been postulated that the insertion of a*dhE* into *C. tyrobutyricum* could create a butanol-producing mutant. Furthermore, it has been shown that deletion of the genes coding for *PTA* and *AK* in *C. tyrobutyricum* significantly increases butyric acid yield compared to the wild type strain [18, 20, 38]. Acetic acid production was not eliminated in these mutants; though it was significantly reduced leading to the postulation that *C. tyrobutyricum* may contain a Co-A Transferase enzyme [38]. The lack of acetone production in *C. tyrobutyricum* also lends to the potential for increased butanol

production because no acetyl-CoA is used to produce this product. Transformation of *adhE* into these mutants could result in a butanol super-producing strain.

2.5: Gene transcription promoters

Gene promoters control the expression of their genes and, in part, the activity of the enzymes the genes code for based on cell environment and stage of growth. Constitutive promoters constantly up-regulate the expression of their genes during all phases of cell growth and in all environments. This results in enzyme activity being regulated by the strength of the promoter and kinetic inhibitors and enhancers present in the cellular environment. Inducible promoters on the other hand are able to up- and down-regulate gene expression based on cell environment and stage of growth, giving a higher degree of control over enzyme activity. The genes responsible for butanol production in ATCC 824, NCIMB 8052, and ATCC 55025 are paired with inducible promoters, up-regulating during the stationary phase of fermentation [12]. Alternatively, the hyper-producing *C. beijerinckii* mutant, BA101, likely has constitutive promoters paired with its butanol producing genes.

It has been shown that the promoter for thiolase, an enzyme in the pathway between acetyl-CoA and butyryl-CoA of both *C. acetobutylicum* and *C. tyrobutyricum*, is a powerful constitutive promoter [30]. Mutants of ATCC 824 created with the thiolase promoter acting on other genes in the pathway were shown to have increased activity of those genes. This promoter has been chosen to accompany *adhE* in the *C. tyrobutyricum* mutant of this research in order to increase potential butanol yield.

Chapter 3: Materials and Methods

3.1: Bacterial strains and plasmids

PCR reactions were performed using *Taq* DNA Polymerase (Platinum® *Taq* DNA Polymerase High Fidelity, Invitrogen 11304-011), which leaves a 5' overhang that is incompatible with restriction enzyme digestion. The t-vector, pGEM-T (pGEM®-T Easy Vector Systems, Promega A1360) was used for ligation and storage of PCR products. This vector is specifically designed to ligate with *Taq* DNA Polymerase. Use of pGEM-T allowed for a continuous strand of DNA that was compatible for digestion.

The final vector containing *adhE* and the thiolase promoter was pMTL007 (Figure 3 on page 14), a conjugation vector designed for gene knockout in species of *Clostridium* [17]. The main features of pMTL007 are the genes ORF H for plasmid replication in species of *Clostridium*, ColE1 for plasmid replication in *E. coli*, *catP* for chloramphenicol resistance, and *traJ* for conjugation in *E. coli*. The other genes within pMTL007 are for gene knockout and were disabled by deletion through digestion.

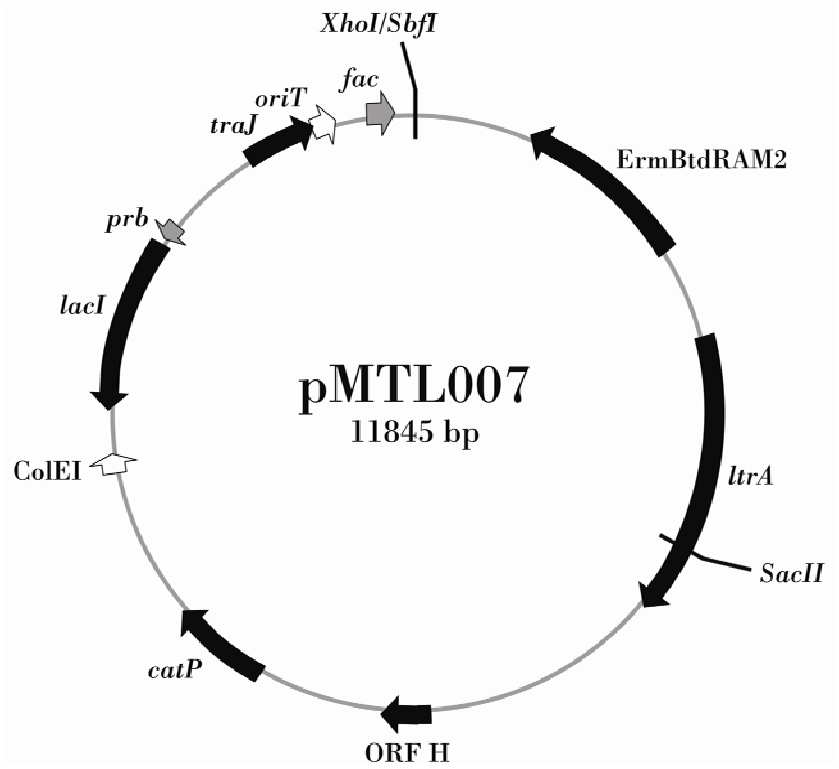

Figure 3. pMTL007 showing restriction sites for promoter and gene insertion.

Clostridium tyrobutyricum ATCC 25755 was the primary bacterial strain used in this study. Its genome was the source of the thiolase promoter. Plasmid amplification and conjugation transformations were performed using *E. coli* strain DH5α (MAX Efficiency® DH5α™ T1 Phage-Resistant Competent Cells, Invitrogen 12034-013). Ligated vectors were transformed into DH5α using heat shock transformation with cell membranes regenerated with S.O.C. Medium (Invitrogen 15544-034). Transformation of the final vector into *C. tyrobutyricum* was performed via conjugation with DH5α. The butanol-producing gene, *adhE*, was isolated from *Clostridium acetobutylicum* ATCC 824. First, *adhE* was amplified from purified ATCC 824 genome, then ligated into the t-vector pGEM-T and transformed into DH5α. This *adhE*-pGEM-T recombinant plasmid was then

used for gene digestion and insertion into pMTL007. A similar process was used for the thiolase promoter. All cells were grown in LB medium (LB Broth, Miller R453642) at a concentration of 2.0 g/L and at 37˚C. Cells were stored in 15% glycerin at -80˚C for up to eight months.

3.2: Restriction sites and primer design

The gene and promoter were ligated into pMTL007 (Figure 3) using single digestion sites found in the plasmid, specifically the restriction sites for enzymes *XhoI*, *SbfI*, and *SacII* (New England BioLabs R01465, R06425, and R0157 respectively). These sites were specifically chosen as sites not located in *adhE*, the thiolase promoter, and pGEM-T and were added onto the ends of the gene and the promoter using custom designed PCR primers. Additionally, all three enzymes operate at 100% in Buffer 4 (NEBuffer 4, New England BioLabs B7004S), allowing multiple digestions to run simultaneously. *XhoI* and *SbfI* are located as depicted in the plasmid, which contains multiple restriction sites for gene insertion. SacII is located in *ItrA* and was chosen to remove ErmBtdRAM2 and *ItrA* from the plasmid, thereby disabling pMTL007's gene knockout capabilities. This span between *XhoI/SbfI* and *ItrA* was the location of *adhE* and promoter insertion. The layout in the final vector was pMTL007-*XhoI*-promoter-*SbfI*-*adhE*-*SacII*-pMTL007 (Figure 4 on page 16).

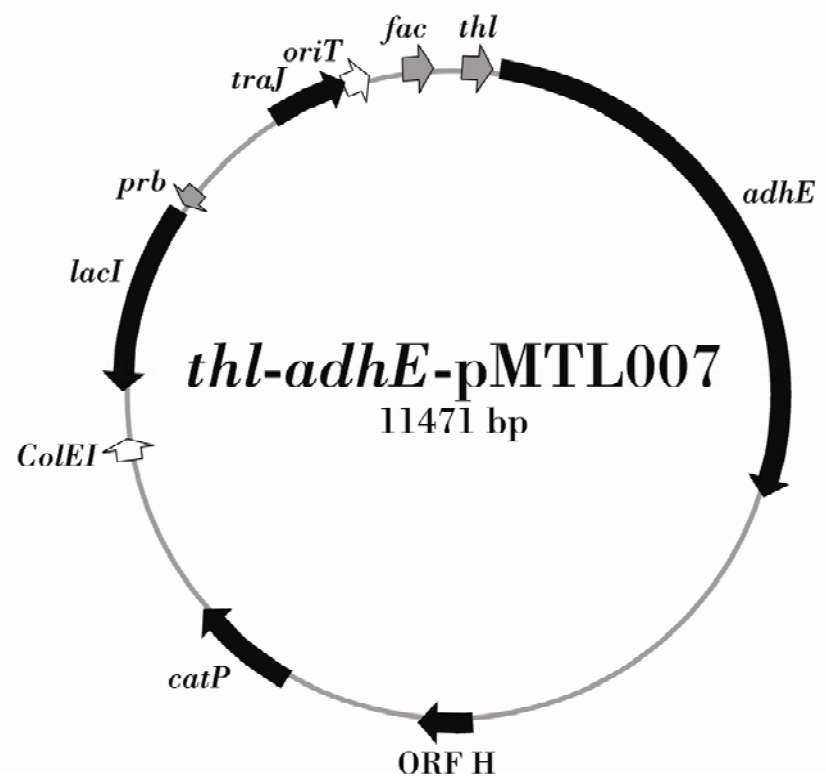

Figure 4. Layout of the final recombinant plasmid *thl-adhE*-pMTL007.

To ensure that the promoter enhanced gene activity most efficiently, the number of base pairs between the thiolase promoter and its native gene was replicated exactly between the promoter and *adhE* in the final ligation product. The sequence between the promoter and its native gene was also replicated exactly, except for where the restriction site was added. The base pairs in this span were added partially to the promoter primer and partially to the gene primer. All primers were designed to have about 50% or more of their sequence coinciding with the template, ensuring full adhesion to the template. These "sticky ends", or the nucleotides of the primer that pair up with the template DNA, cover from about 20 to 30 nucleotides into the template and end at the beginning of the restriction sites. The "overhang ends", or the

nucleotides of the primer that do not adhere to the template, contain the restriction sites plus an extra four nucleotides on the end. The last four nucleotides are necessary for proper restriction enzyme activity. Nucleotides for this section were designed to ensure proper GC content within the primer in accordance with the primer design guidelines defined by Invitrogen.

The primers for *adhE*, labeled ForAAD for forward transcription and RevAAD for reverse transcription, were designed with restriction sites for SbfI and SacII, respectively. The sequences for both are shown in Figure 5. ForAAD contains the *SbfI* site and has a GC content of 36.1% and is 54.1% overhang. The length of the sticky end was determined based on the required length of the overhang while optimizing GC content. This primer contains part of the sequence that lies between the promoter and its native gene, resulting in the large overhang percentage. The large size of ForAAD, 61 nucleotides, ensured that the sticky end would be long enough to overcome the size of the overhang. RevAAD contains the *SacII* site and has a GC content of 29.3% and is 24.4% overhang. The overhang is entirely comprised of the restriction site and the final four nucleotides for maximum adhesion because there is no length requirement after the

ForAAD
5'-CTAT**CCTGCA'GG**AAATATTTAGGAGGAATAGTC*ATG*AAAGTCACAACAGTAAAGGAATTAG-3'
SbfI

RevAAD
5'-GATT**CCGC'GG**TTAAGGTTGTTTTTTAAAACAATTTATATAC-3'
SacII

Figure 5. Sequences of ForAAD and RevAAD. Restriction sites are in bold and underlined with their labels below the site. Restriction points shown with an apostrophe. The start codon is italicized and underlined.

end of the gene. The length of the sticky end was chosen to optimize both primer length and GC content.

Primers for the thiolase promoter were labeled similarly to those of *adhE* (Figure 6). ForTHL contains the *XhoI* restriction site. It contains a GC content of 40.0% and is 33.3% overhang. Like RevAAD, there is no length requirement before the beginning of the promoter, so the overhang is entirely comprised of the restriction site and the final four nucleotides. Again, the length of the sticky end was chosen to optimize primer length and GC content. RevTHL contains both the *SbfI* and *SacII* restriction sites and is the point at which *adhE* was eventually ligated to complete the final recombinant vector. This primer has a GC content of 41.5% and is 43.4% overhang. The overhang end contains the rest of the sequence that lies between the promoter and its native gene that is not contained by ForAAD.

3.3: DNA amplification, digestion, purification, and ligation

Amplification of *adhE* and the thiolase promoter was performed using Platinum® *Taq* DNA Polymerase High Fidelity (Invitrogen 11304-011) and the custom designed primers

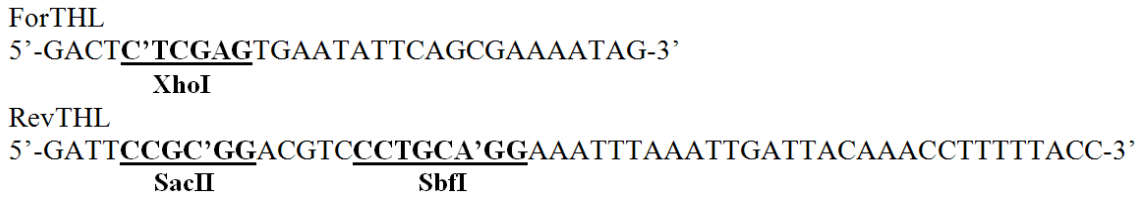

Figure 6. Sequences of ForAAD and RevAAD. Restriction sites are in bold and underlined with their labels below the site. Restriction points shown with an apostrophe.

with restriction enzyme sites included. The reaction was set up as described in the Invitrogen protocol with 35 rounds of amplification. The reaction products were run on agarose gel to verify DNA amplification, and then purified using the QIAquick PCR Purification Kit (QIAGEN 28104) before ligation into pGEM-T. Ligation was performed with T4 DNA Ligase (Promega M180A) using 50 ng of pGEM-T at an insert to vector molar ratio of 3:1 as described in the protocol provided by Promega.

Amplification of the pGEM-T-PCR product recombinant vectors was accomplished by transformation into DH5α cells. These cells were grown for 16 hours on LB medium plates, utilizing the cells' enzymes to amplify the plasmid within each cell. Ampicillin (100 μg/ml), IPTG (95.2 μg/ml), and X-gal (80 μg/ml) were mixed into the growth medium to select for cells containing the recombinant vector. pGEM-T contains a gene for ampicillin resistance, so cells that did not take up a vector were not able to grow. IPTG and X-gal further separated between cells with recombinant vectors and cells with pGEM-T, but no ligated PCR product. This is dictated by the pGEM-T ligation and cell transformation protocol where blue colonies do not contain the recombinant vector and white colonies do. PCR was used to verify the existence of the recombinant vector within white colonies using the same reaction setup as for gene and promoter amplification with the DNA template replaced by a fraction of the colony. After the recombinant plasmid was verified to exist within the cells of a certain colony, that colony was extracted from the plate and grown in liquid LB medium with ampicillin for 16 hours. Finally, the plasmid was purified from the liquid colony using the QIAprep

Spin Miniprep Kit (QIAGEN 27104). Purification of the correct plasmid was confirmed by checking the size on agarose gel. The plasmid was then digested with *XhoI*, *SbfI*, or *SacII* (whose restriction sites only occur in the added primer regions) and, again, the size was checked on agarose gel.

To prepare pMTL007 and the recombinant plasmids containing *adhE* and the thiolase promoter for ligation, they were double-digested with the appropriate restriction enzymes. The promoter was ligated into pMTL007 first, so each were digested with XhoI and SacII for about 3 hours at 37°C. Digestion progress was confirmed at 2.5 hours by checking on agarose gel before denaturing the enzymes for 20 minutes at 65°C. Agarose gel was then used to separate the digested DNA fragments, which were cut from the gel and purified with the QIAquick Gel Extraction Kit (QIAGEN 28704). Purified digestion product concentrations were checked with a spectrophotometer (Thermo Scientific NanoDrop ND-1000). Work continued only if the concentration of each was at least 10 ng/µl. Otherwise, the vector was digested again and the new digestion product was added to the previous product and concentrated with the PCR purification kit. This process was repeated as needed until the aforementioned concentration was reached.

Once each digestion product was at the appropriate concentration, the segments were ligated with T4 DNA Ligase (New England BioLabs M0202S) overnight at 4°C at an insert to vector molar ratio of 4:1 and a total DNA concentration of 10 ng/ml. The pMTL007-promoter recombinant plasmid was amplified in DH5α in similar fashion as the

amplification of the pGEM-T recombinant plasmids using chloramphenicol (30 μg/ml) as the antibiotic selector. After purification from the liquid colonies, the plasmid was verified with agarose gel and single digestion with SbfI, whose restriction site was present only in the inserted promoter region.

The *thl*-pMTL007 recombinant plasmid was digested with *SbfI* and *SacII* using the same protocol as for promoter digestion. The gene was digested from pGEM-T in the same fashion, except for the addition of the restriction enzyme *XmnI* (New England BioLabs R0194S). The *XmnI* restriction site is located 1000 bp from the ligation site in pGEM-T and is not present in *adhE*. Since pGEM-T and *adhE* have similar lengths, digestion with *XmnI* was used to break up the vector segment for differentiation between the gene and vector. The digestion products were separated on agarose gel, and then purified as before. After bringing the concentrations of each product to 10 ng/μl by the same method as with the previous digestion, *adhE* and the pMTL007-promoter vector were ligated at an insert to vector ratio of 3:1 with T4 DNA Ligase as before. The lower ratio was used because of the size of the *adhE* insert. This final recombinant plasmid was amplified using DH5α, again with chloramphenicol for antibiotic selection.

3.4: Vector transformation

Two kinds of vector transformation were used in this research: heat shock and conjugation. Heat shock was used when vectors were to be amplified using DH5α cells

and conjugation was used for transforming the final recombinant plasmid from DH5α to *C. tyrobutyricum*.

Transformation by heat shock was performed using 50 µl of DH5α cells and 10 µl of ligation product. Ice cold cells and product were mixed together and placed on ice for 30 minutes. The mixture was then heat shocked for one minute at 42˚C, then placed back on ice for five minutes. It was then mixed with 240 µl of S.O.C. Medium (Invitrogen 15544-034) and agitated at 250 rpm for 60 minutes at 37˚C. Finally, the mixture was spread onto LB medium plates with the appropriate antibiotic and, for pGEM-T transformations, IPTG and X-gal. The mixture was spread onto four different plates, one plate was streaked and the other three received 20, 40, and 200 µl aliquots. Plates were incubated for 16 hours. All mixing of cells, in addition to spreading the mixture onto plates, was performed over a flame from a Bunsen burner for sterility. The overall process of recombinant plasmid creation is diagramed in Figures 7-9 on pages 23-25.

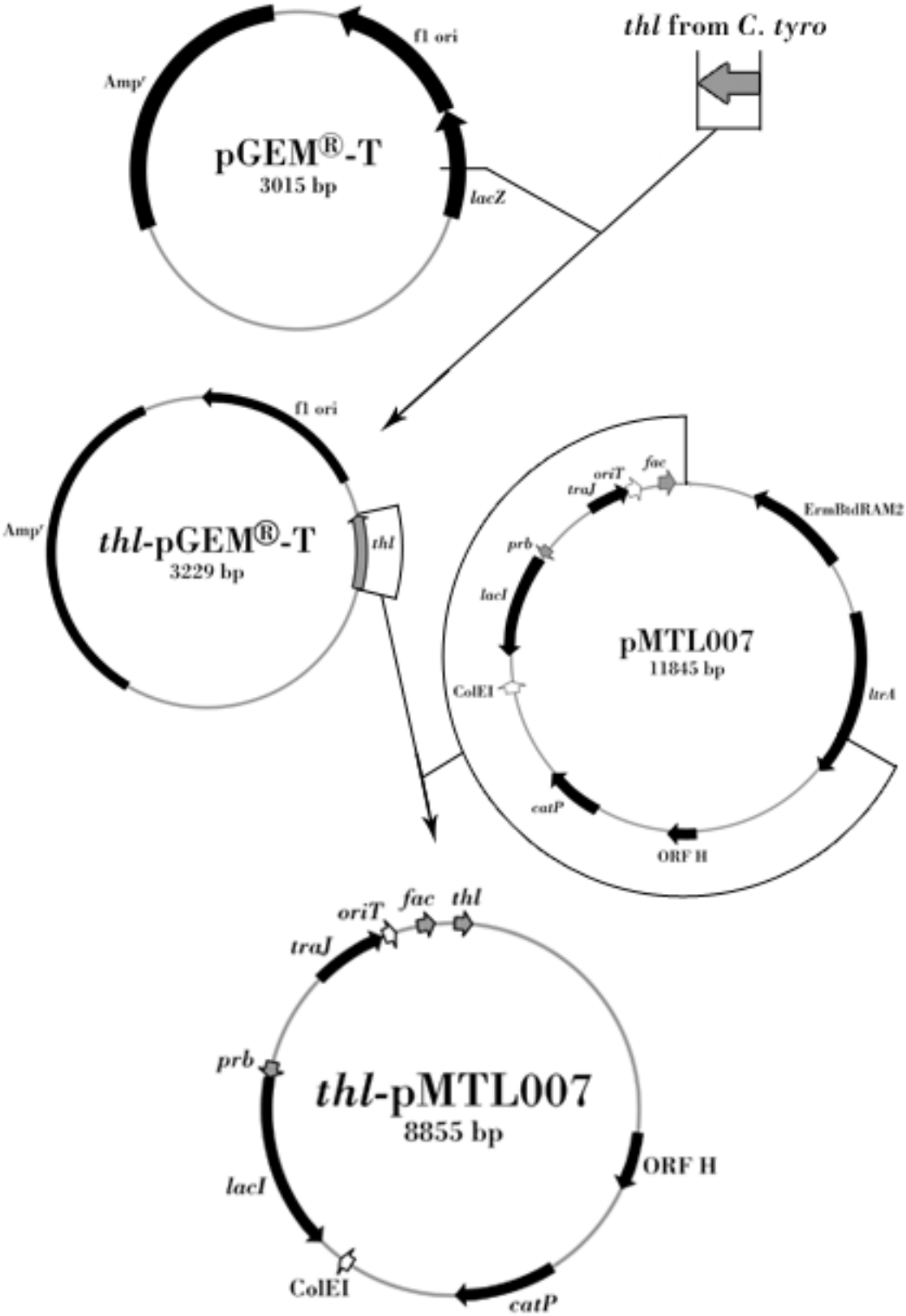

Figure 7. Diagram depicting the creation of the *thl*-pMTL007 recombinant plasmid starting from the *Clostridium tyrobutyricum* genome.

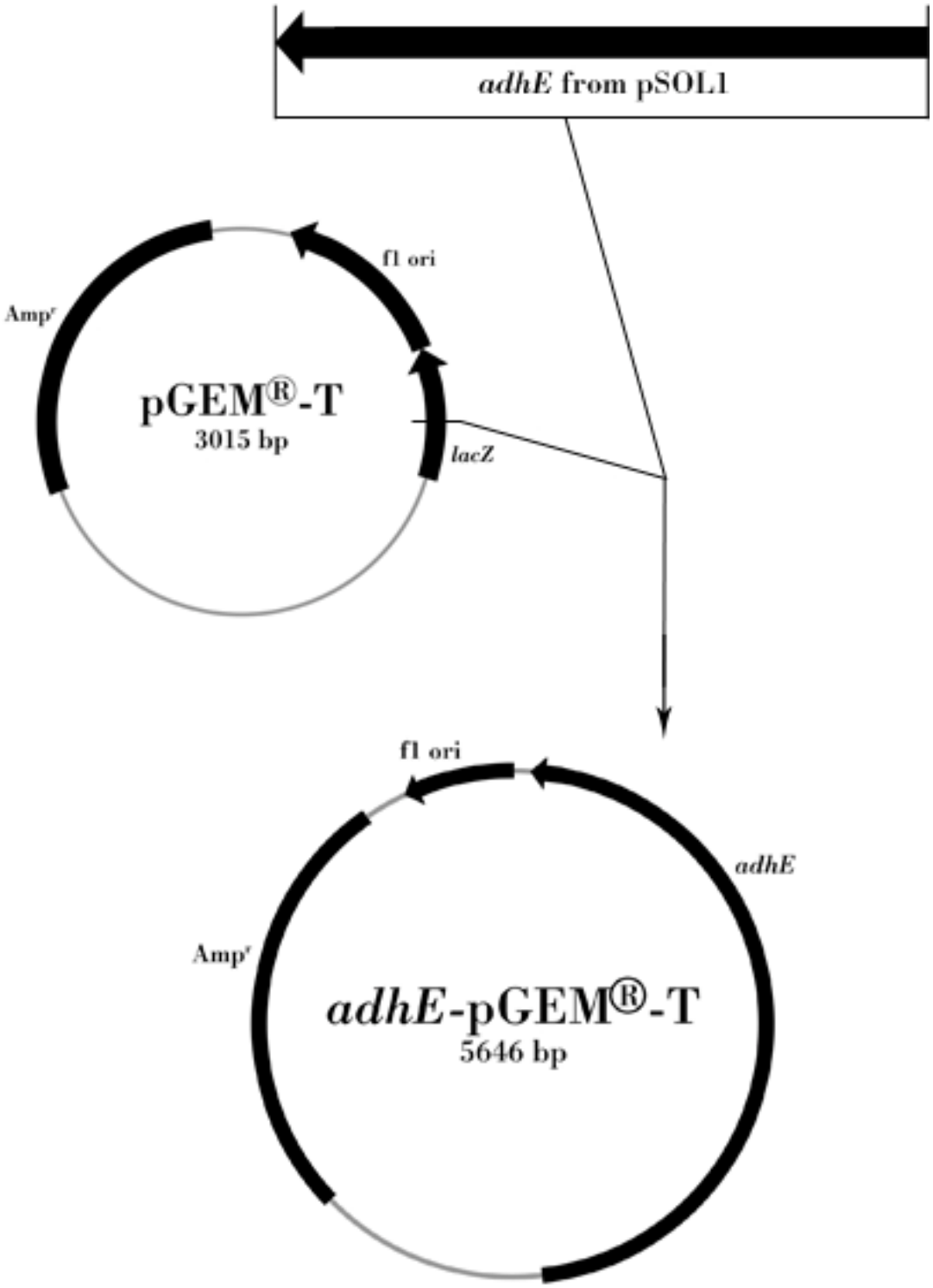

Figure 8. Diagram depicting the creation of the *adhE*-pGEM-T recombinant plasmid starting with pSOL1 from *Clostridium acetobutylicum*.

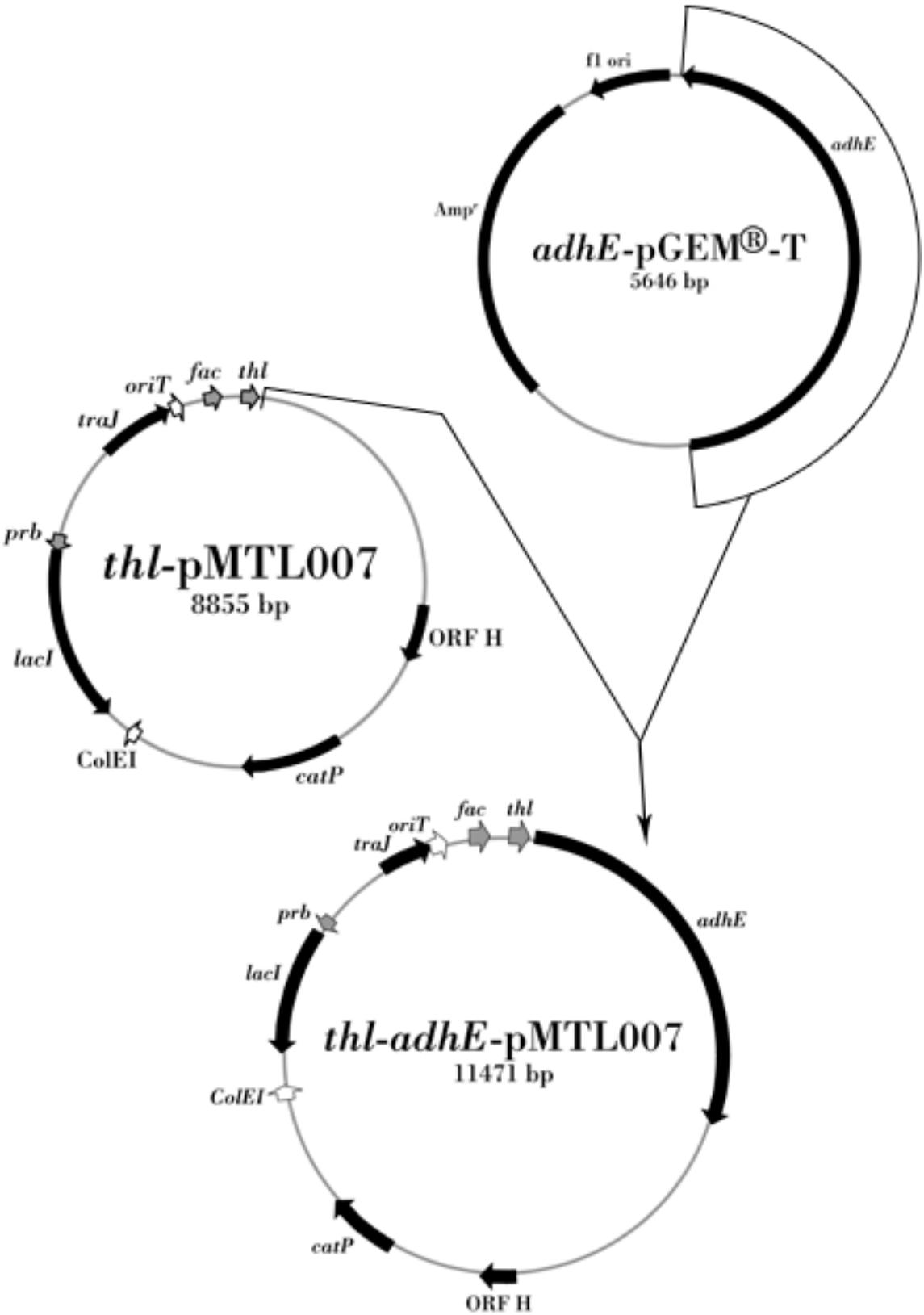

Figure 9. Diagram depicting the creation of the *thl-adhE*-pMTL007 recombinant plasmid.

Chapter 4: Results and Discussion

Initial amplifications of the thiolase promoter using the *C. tyrobutyricum* genome as the template were only marginally successful. While the amplified DNA from both the genome amplifications and the colony amplifications after ligation with pGEM-T were visible on the gels, digestion from pGEM-T yielded very low concentrations that could not be used in ligation with pMTL007. This suggested that the amplification yield using the genome template was too low to obtain good results with pGEM-T. The template was changed to a recombinant plasmid containing the promoter and *adhE2*, which yielded much better results (Figure 10).

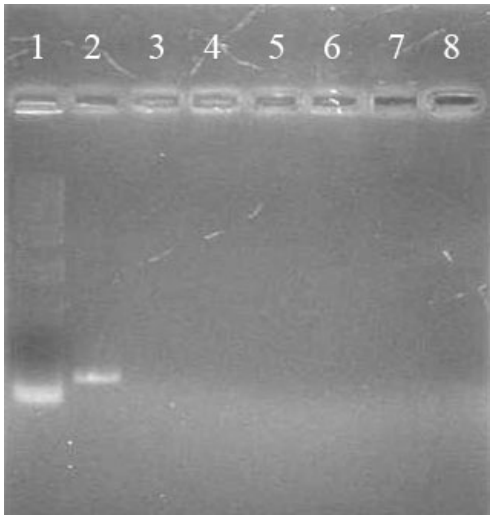

Figure 10. PCR amplification of the thiolase promoter. Lane 1 is the sizing ladder, lane 2 is the promoter, and all other lanes are empty.

Overnight ligation of this amplification product into pGEM-T and transformation into DH5α cells resulted in good growth on all LB plates. Ten of the white colonies were picked for PCR amplification to verify the presence of the promoter. There were three colonies each picked from the streaked plate and the 20 µl plate, and two each from the other plates. Of the ten colonies selected, only five tested positive for containing the promoter (Figure 11). Colonies 5, 7, 8, and 10 (lanes 6, 8, 9, and 11) were selected for growth in liquid medium because of their high visibility on the gel, suggesting a higher concentration of recombinant plasmid within those colonies.

Each colony grew successfully overnight in the liquid medium. The recombinant plasmids were recovered from the colonies using the QIAprep Spin Miniprep Kit (QIAGEN 27104) and the purified products were combined into one solution. This

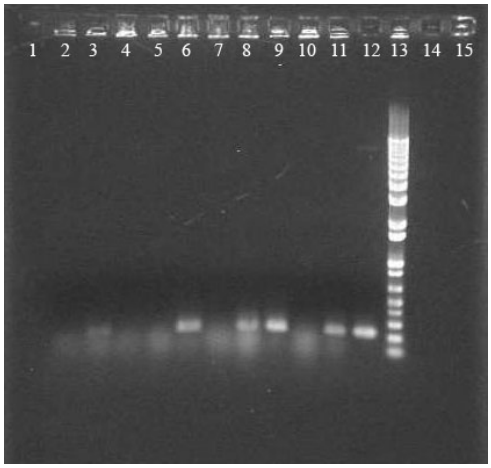

Figure 11. Colony PCR of the thiolase promoter. Lane 1 is the negative control, lanes 2-11 are the colonies, lane 12 is the positive control, lane 13 is the sizing ladder, and the other lanes are empty.

solution was digested with *XhoI* and *SacII*, as was pMTL007, using 40 µl of DNA solution in a 100 µl reaction (Figure 12). Purification of the 8 kb segment from the two lanes of pMTL007 yielded concentrations of 16.4 and 22.8 ng/µl, well above the required concentration of 10 ng/µl. However, the purified promoter resulted in concentrations of 6.3, 7.1, and 6.9 ng/µl, so the results from the three lanes were combined and concentrated using the QIAquick PCR Purification Kit (QIAGEN 28104). The new concentration was still too low at 7.4 ng/µl. The promoter was re-digested from pGEM-T, this time using 55 µl of DNA solution (Figure 13). Purification of this digestion product yielded concentrations of 4.2, 4.9, and 13.2 ng/µl. The latter was suitable for transformation and was used for ligation with pMTL007.

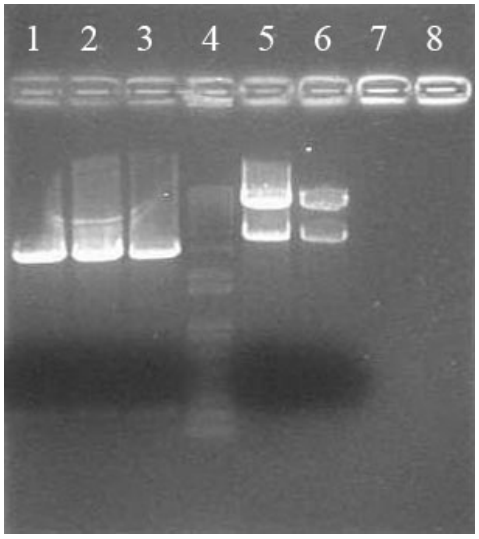

Figure 12. Digestion of the thiolase promoter and pMTL007 with *XhoI* and *SacII*. Lanes 1-3 are the promoter, lane 4 is the sizing ladder, lanes 5 and 6 are pMTL007, and lanes 7 and 8 are empty.

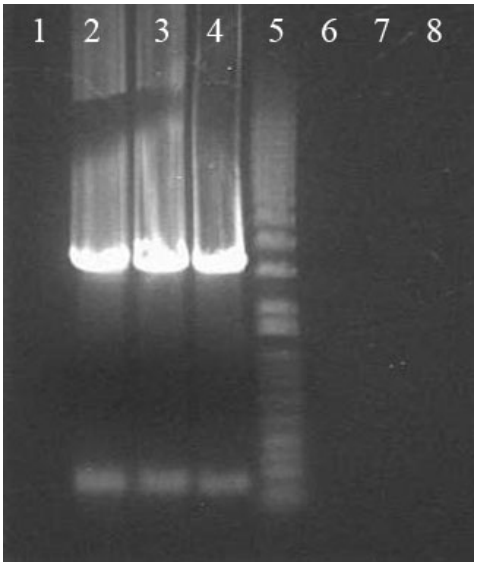

Figure 13. Second digestion of the thiolase promoter with *XhoI* and *SacII*. Lanes 2-4 are the promoter, lane 5 is the sizing ladder, and the other lanes are empty.

The ligation of the promoter into pMTL007 and subsequent transformation into DH5α cells has thus far been unsuccessful. There is need to optimize both processes simultaneously on the basis of reactant concentrations and vector to cell ratio. A full factorial experimental design has been created with three levels each on total vector concentration during ligation and vector dilution during transformation (Table 4). This design can be easily expanded to include other factors by blocking if needed. Optimization is based on cell count at the end of transformation.

Table 4. Full factorial experimental layout for optimizing the ligation and transformation process.

Run	Pattern	Total DNA Concentration (ng/μl)	Vector Dilution (% Vector Solution by Volume)
1	23	30	15
2	31	50	2
3	33	50	15
4	31	50	2
5	23	30	15
6	11	10	2
7	12	10	10
8	21	30	2
9	33	50	15
10	11	10	2
11	13	10	15
12	22	30	10
13	21	30	2
14	32	50	10
15	22	30	10
16	13	10	15
17	32	50	10
18	12	10	10

The gene was amplified and ligated into pGEM-T at the same time as the promoter. Amplification of *adhE* from the *C. acetobutylicum* genome was unsuccessful at first, yielding no results. Using the knowledge gained from amplification of the promoter, I located a stock of *adhE* ligated into pGEM-T with different restriction sites on the ends. This plasmid was used as the PCR template with the ForAAD and RevAAD primers, resulting in successful amplification (Figure 14).

Ligation into pGEM-T resulted in excellent growth on the LB plates. Again, ten colonies were selected in the same manner as the promoter and checked via PCR for the presence of *adhE*. All ten colonies were found to contain the gene (Figure 15), so the four best amplification results (on the basis of visibility on the gel) were used as the selections to grow liquid colonies. Each of the liquid colonies grew successfully and the

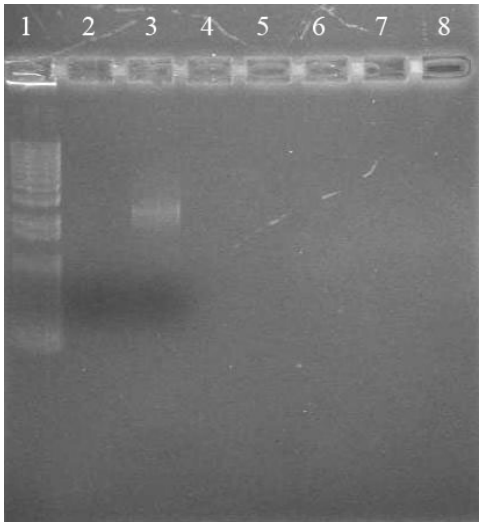

Figure 14. PCR amplification of *adhE*. Lane 1 is the sizing ladder, lane 2 is a failed amplification, lane 3 is a successful amplification, and the other lanes are empty.

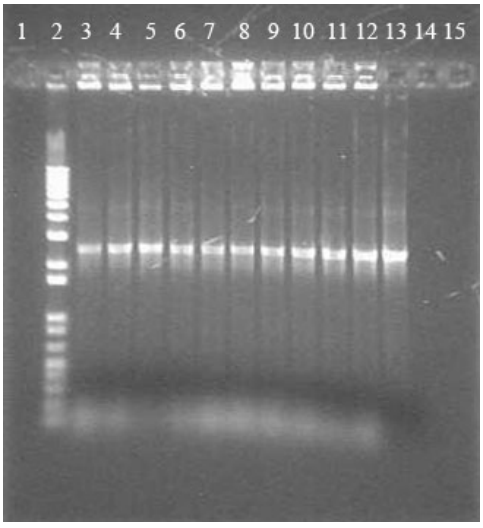

Figure 15. Colony PCR of <u>*adhE*</u>. Lane 2 is the sizing ladder, lanes 3-12 are the colonies, lane 13 is the positive control, lane 14 is the negative control, all other lanes are empty.

plasmid was extracted using the QIAprep Spin Miniprep Kit (QIAGEN 27104), combining the solutions to store at -20˚C until needed for digestion.

Chapter 5: Conclusions

While the plasmid was not completed and transformed into *C. tyrobutyricum*, it is reasonable to assume that this gene, once inserted, will enable the mutant strain to produce butanol. *C. tyrobutyricum* shares many similarities with the source strain of *adhE*: *C. acetobutylicum* ATCC 824. They have metabolic pathways that are identical in function from pyruvate through butyryl-CoA and have high metabolic flux from acetyl-CoA through butyryl-CoA due to thiolase and its promoter [30].

One possible drawback to butanol production using *adhE* is the active pH. Maximum butyric acid production in *C. tyrobutyricum* occurs at pH 6.3 [37], whereas maximum *adhE* activity in *C. acetobutylicum* occurs at pH 4.4 [11]. Use of the constitutive thiolase promoter ensures that translation of *adhE* will occur regardless of the cellular environment. However, it is unclear whether pH effects gene transcription or enzyme activity within the ATCC 824 wild type. If only transcription is effected, then the difference in pH will not be a problem when using the thiolase promoter. The interaction of pH and *adhE* can be studied upon fermentation of *C. tyrobutyricum*.

Use of a *C. tyrobutyricum* mutant containing *adhE* and with inactivated *PTA* or *AK* could also produce high concentrations of butanol when fermented at or below pH 5.0,

especially with the decreased levels of acetic acid production [18, 20, 38]. However, due to the activity of the unknown acetyl-CoA producing enzyme in *C. tyrobutyricum*, the production levels of butanol and ethanol may still be comparable at best when using either the *PTA* or *AK* deletion mutant.

Testing of these hypotheses can begin as soon as the recombinant plasmid is completed and transformed into *C. tyrobutyricum* and its mutants. The ligation and transformation processes should be easily optimized using a full factorial experimental design, allowing completion of plasmid construction. Furthermore, detailed investigation into the genome of *C. tyrobutyricum* should reveal the other gene(s) responsible for acetic acid production in the wild type. This gene could be inactivated along with *PTA* and *AK* in a single mutant, eliminating acetic acid production and causing all acetyl-CoA to be metabolized into butyryl-CoA. Fermentation of this mutant at the optimal pH for *adhE* is likely to produce a higher yield of butanol.

Finally, insertion of both *adhE* and *adhE2* would likely result in a mutant able to produce butanol in multiple fermentation conditions. Since *adhE2* is most active near neutral pH [11], as is butyric acid production in wild type *C. tyrobutyricum* [37], the strain would operate under alcohologenisis during most of fermentation, but fluctuations in pH would activate *adhE*, enabling the strain to produce butanol through a wider pH range. This would also allow for relaxed controls on pH in an industrial setting, reducing both

energy and material costs, thus making butanol production with this strain even more energy efficient.

Chapter 6: Future Work

After optimization of the ligation and transformation protocols, the final recombinant plasmid needs to be constructed and transformed via conjugation into *C. tyrobutyricum*. The strain then needs to be fermented in order to confirm its butanol production capabilities. Fermentation using the insertion mutant with no mutations otherwise must be completed before any further work can be conducted. Fermentation should first be conducted using pure glucose at a concentration of 6% with pH controlled at 4.4 to induce the solventogenic conditions in which *adhE* produces butanol in *C. acetobutylicum* [11].

After confirmation of ability to produce butanol, the next task is to enhance and optimize the strain's butanol producing capabilities. A wide variety of factors must be tested in this stage, including investigating other gene promoters, creation of recombinant vectors using other source vectors, and optimization of nutrient concentrations and growth conditions. Since each combination of promoter, plasmid, and gene is likely to have different optimized growth conditions, the original mutant strain's optimized growth conditions cannot be assumed to be optimal for other mutant strains. The most efficient and accurate way to test each of these variables is to first

verify the butanol producing capabilities of each mutant strain, then test them all in parallel using a fully randomized fractional factorial experimental design.

Finally, after a full investigation into the effects detailed above, a mutant can be constructed using both *adhE* and *adhE2* to investigate the butanol production capabilities of a mutant strain capable of butanol production in a wide pH range. Similar studies to those detailed above can be conducted to investigate the effects of various promoters, plasmids, and growing conditions.

References

[1] 1-Butanol. International Chemical Safety Card 0111. Geneva: International Labour Organization, 2005.

[2] AAA. AAA's Daily Fuel Gauge Report. 3 May 2010. 3 May 2010 <http://www.fuelgaugereport.com/>.

[3] Argonne National Lab. Lower-Higher Heating Values. 5 September 2008. 12 April 2010 <http://webcache.googleusercontent.com/search?q=cache:OtsrLVxIoKgJ:hydrogen.pnl.gov/filedownloads/hydrogen/datasheets/lower_and_higher_heating_values.xls+argonne+national+lab+lower-higher+heating+values&cd=1&hl=en&ct=clnk&gl=us>.

[4] Awang, Gregor M., G. A. Jones and W. M. Ingledew. "The Acetone-Butanol-Ethanol Fermentation." Critical Reviews in Microbiology 15.1 (1988): S33-S67.

[5] Chen, C. K. and H. P. Blaschek. "Acetate Enhances Solvent Production and Prevents Degeneration in Clostridium beijerinckii BA101." Applied Microbiology and Biotechnology 52 (1999): 170-173.

[6] Energy Literacy. Energy Primer 101. 2007. 5 March 2010 <http://energyliteracy.org/energy_101.html>.

[7] Ethanol (Anhydrous). International Chemical Safety Card 0044. Geneva: International Labour Organization, 2000.

[8] Evans, Michael K. "The Economic Impact of the Demand for Ethanol." Final Report. Midwestern Governors' Conference, 1997.

[9] Fan, L.-S., P. Gupta and L. Vargas. Methods for Making Hydrogen from Gaseous and Solid Carbonaceous Fuels. United States Provisional Patent: Patent 60/758507. 2006.

[10] Fischer, Ralf J., Jan Helms and Peter Durre. "Cloning, Sequencing, and Molecular Analysis of the sol Operon of Clostridium acetobutylicum, a Chromosomal Locus Involved in Solventogenesis." Journal of Bacteririology 175.21 (1993): 6959-6969.

[11] Fontaine, Lisa, et al. "Molecular Characterization and Transcriptional Analysis of adhE2, the Gene Encoding the NADH-Dependent Aldehyde/Alcohol Dehydrogenase Responsible for Butanol Production in Alcohologenic Cultures of Clostridium acetobutylicum ATCC 824." Journal of Bacteriology 184.3 (2002): 821-830.

[12] Formanek, Joseph, Roderick Mackie and Hans P. Blaschek. “Enhances Butanol Production by Clostridium Beijerinckii BA101 Grown in Semidefined P2 Medium Containing 6 Percent Maltodextrin or Glucose.” Apply and Environmental Microbiology 63.6 (1997): 2306-2310.

[13] Gasoline. International Chemical Safety Card 1400. Geneva: International Labour Organization, 2001.

[14] Gholizadeh, Laili. “Enhanced Butanol Production by Free and Immobilized Clostridium sp. Cells Using Butyric Acid as Co-Substrate.” Master Thesis. University of Boras, 2009.

[15] Global Greenhouse Warming. Ethanol Biofuel. 2 May 2010. 2 May 2010 <http://www.global-greenhouse-warming.com/ethanol-biofuel.html>.

[16] Green, Don W. and Robert H. Perry. Perry's Chemical Engineers' Handbook, 8th ed. New York: McGraw-Hill, 2008.

[17] Heap, John T., et al. “The ClosTron: A Universal Gene Knock-out System for the Genus Clostridium.” Journal of Microbiological Methods 70 (2007): 452-464.

[18]Liu, Xiaoguang, Ying Zhu and Shang-Tian Yang. “Construction and Characterization of ack Deleted Mutant of Clostridium tyrobutyricum for Enhanced Butyric Acid and Hydrogen Production.” Biotechnology Progress 22 (2006): 1265-1275.

[19] Liu, Ziyong, et al. “Butanol Production by Clostridium beijerinckii ATCC 55025 from Wheat Bran.” Journal of Industrial Microbiology and Biotechnology (2010).

[20] Lui, Xiaoguang, Ying Zhu and Shang-Tian Yang. “Butyric Acid and Hydrogen Production by Clostridium tyrobutyricum.” Enzyme and Microbial Technology 38 (2006): 521-528.

[21] Nair, Ramesh V. and Eleftherios T. Papoutsakis. “Expression of Plasmid-Encoded aad in Clostridium acetobutylicum M5 Restores Vigorous Butanol Production.” Journal of Bacteriology 176.18 (1994): 5843-5846.

[22] NIST. 1-Butanol. 1 August 2008. 5 May 2010 <http://webbook.nist.gov/cgi/cbook.cgi?Name=butanol&Units=SI>.

[23] Nolling, Jork, et al. “Genome Sequence and Comparative Analysis of the Solvent-Producing Bacterium Clostridium acetobutylicum.” Journal of Bacteriology 183.16 (2001): 4823-4838.

[24] Ohta, Kazuyoshi, et al. “Genetic Improvement of Escherichia coli for Ethanol Production: Chromosomal Integration of Zymomonas mobilis Genes Encoding Pyruvate Decarboxylase and Alcohol Dehydrogenase II.” Applied and Environmental Microbiology 57.4 (1991): 893-900.

[25] PBS. Timeline: History of the Electric Car. 30 October 2009. 7 March 2010. <http://www.pbs.org/now/shows/223/electric-car-timeline.html>.

[26] Ramey, David and Shang-Tian Yang. “Production of Butyric Acid and Butanol from Biomass.” Final Report. 2004.

[27] ScienceDaily. Ethanol and Biodiesel from Crops Not Worth the Energy. 6 July 2006. 14 April 2010 <http://www.sciencedaily.com/releases/2005/07/050705231841.htm>.

[28] Scotcher, Miles C., et al. "Sequences Affecting the Regulation of Solvent Production in Clostridium acetobutylicum." Journal of Industrial Microbiology and Biotechnology 30 (2003): 414-420.

[29] Shi, Zhen and Hans P. Blaschek. "Transcriptional Analysis of Clostridium beijerinckii NCIMB 8052 and the Hyper-Butanol-Producing Mutant BA101 During the Shift from Acidogenesis to Solventogenesis." Applied and Environmental Microbiology 74.24 (2008): 7709-7714.

[30] Sillers, Ryan, Mohab Ali Al-Hinai and Eleftherios T. Papoutsakis. "Aldehyde-Alcohol Dehydrogenase and/or Thiolase Overexpression Coupled with CoA Transferase Downregulation Lead to Higher Alcohol Titers and Selectivity in Clostridium acetobutylicum Fermentations." Biotechnology and Bioengineering 102.1 (2009): 38-49.

[31] The Fraser Domain. IEO2007: Liquid Fuels. 24 May 2007. 5 March 2010 <http://thefraserdomain.typepad.com/energy/2007/05/ieo2007_use_of.html>.

[32] Tummala, Seshu B., Neil E. Welker and Eleftherios T. Papoutsakis. "Development and Characterization of a Gene Expression Reporter System for Clostridium acetobutylicum ATCC 824." Applied and Environmental Microbiology 65.9 (1999): 3793-3799.

[33] Tummala, Sheshu B., et al. "Transcriptional Analysis of Product-Concentration Driven Changes in Cellular Programs of Recombinant Clostridium acetobutylicum Strains." Biotechnology and Bioengineering 84.7 (2003): 842-854.

[34] UNCTAD. Market Structure: Paladium. 7 March 2010 <http://www.unctad.org/infocomm/anglais/palladium/chain.htm>.

[35] Weizmann, Charles. Production of Acetone and Alcohol by Bacteriological Processes. United States of America: Patent 1315585. 1919 йил 9-September.

[36] Wu, Zetang and Shang-Tian Yang. "Extractive Fermentation for Butyric Acid Production from Glucose by Clostridium tyrobutyricum." Biotechnology and Bioengineering 82.1 (2003): 93-102.

[37] Zhu, Ying and Shang-Tian Yang. "Effect of pH on Metabolic Pathway Shift in Fermentation of Xylose by Clostridium tyrubutyricum." Journal of Biotechnology 110 (2004): 143-157.

[38] Zhu, Ying, Xiaoguang Liu and Shang-Tian Yang. "Construction and Characterization of pta Gene-Deleted Mutant of Clostridium tyrobutyricum for Enhanced Butyric Acid Fermentation." Biotechnology and Bioengineering 90.2 (2005): 154-166.

Appendix: Reaction Protocols

Table 5. PCR protocol as called for by protocol for Platinum® *Taq* DNA Polymerase High Fidelity. DNA template is replaced by cell colony for colony PCR.

Component	Volume (µl)
10x High Fidelity PCR Buffer	5
10 mM dNTP	1
50 mM $MgSO_4$	2
Forward Primer	2
Reverse Primer	2
DNA Template	1
Platinum® *Taq* High Fidelity	0.2
Sterilized H_2O	36.8
Total	50

Table 6. Temperature cycle for PCR with Platinum® *Taq* DNA Polymerase.

Step	Temperature (˚C)	Time	Cycles
Initial Denature	94	2 min	1
Denature	94	30 s	35
Anneal	55	30 s	
Extend	68	45 s	
Final Extend	68	10 min	1
End Reaction	10	∞	1

Table 8. Ligation of promoter PCR product with pGEM®-T vector.

Component	Volume (µl)
2x Rapid Ligation Buffer	25
pGEM®-T Easy Vector	5
thl PCR Product	1.5
T4 DNA Ligase	5
Sterilized H_2O	13.5
Total	50

Table 7. Ligation of gene PCR product with pGEM®-T vector.

Component	Volume (µl)
2x Rapid Ligation Buffer	25
pGEM®-T Easy Vector	5
adhE PCR Product	5.8
T4 DNA Ligase	5
Sterilized H_2O	9.2
Total	50

Table 9. Protocol for transformation of all ligation products into DH5 cells. Transformation product was plated and grown as described in Chapter 3.

10 µl	Ligation Product
50 µl	DH5α Cells
Ice	30 min
42˚C	1 min
Ice	5 min
250 µl	S.O.C. Medium
37˚C	Shake at 250 rpm for 1 hr

Table 10. Protocol for digestion of pGEM®-T ligation products and pMTL007. *For thiolase promoter, use 55 µl.

Component	Volume (µl)
NEBuffer 4	10
Enzyme	2 each
DNA	40*
Sterilized H_2O	to 100

Table 11. Protocol for ligation of thiolase promoter with pMTL007. This protocol is still being optimized.

Compontent	Volume (µl)
T4 DNA Ligase Reaction Buffer (10x)	2
thl Insert	3.5
pMTL007 Vector	13.5
T4 DNA Ligase	1
Total	20

Table 12. Protocol for making LB plates. *Components only used with pMTL007 recombinant plasmids. **Components only used with pGEM®-T recombinant plasmids.

Ingrediant	Concentration
LB Broth	20 mg/ml
Granulated Agar	15 mg/ml
Chloramphenicol*	30 µg/ml
Ampicillin**	100 µg/ml
IPTG**	95.2 µg/ml
X-Gal**	80 µg/ml